ASME-ATI-UIT 2015 Conference on Thermal Energy Systems: Production, Storage, Utilization and the Environment
17 – 20 May, 2015, Napoli, Italy

DESTRUCTIVE EFFECT OF CONSTANT-HEIGHT PIN FIN HEAT SINKS ON TEMPERATURE UNIFORMITY OF LITHIUM-ION BATTERIES

Shahabeddin K. Mohammadian, Yuwen Zhang*

Department of Mechanical and Aerospace Engineering, University of Missouri, Columbia, MO 65211, USA

ABSTRACT

Three dimensional transient thermal analysis of an air-cooled module was studied for thermal management of the Li-ion (Lithium-ion) battery pack. The module contains the prismatic Li-ion cells and a heat sink with or without pin fins. The effects of pin fins, state of charge, and discharge rate on the battery were investigated and the results showed that using constant-height pin fins increases the standard deviation of the temperature field; however, they decrease the temperature inside the battery significantly. Since thermal management of Li-ion batteries should improve the temperature uniformity inside the battery, the use of this kind of pin fin heat sinks (constant height) is not beneficial for Li-ion batteries. Decreasing the state of charge and increasing the discharge rate cause to increase both the temperature and the standard deviation of the temperature field inside the battery for both cases of with and without pin fins.

Keywords: Lithium-ion battery pack, Thermal management, Pin fin heat sink, Hybrid electric vehicles.

INTRODUCTION

Depleting fossil fuels and their destructive effects on environmental pollution is one of the main challenges in the automotive industry. Electric vehicles (EVs) and hybrid electric vehicles (HEVs) have attracted more attentions for the purpose of energy saving and also environmental protection [1]. Li-ion batteries are preferred for electric and hybrid electric vehicles, because of high energy density and long cycle life. In addition, they are generally safe and do not suffer from memory effects [2]. Heat generation inside the Li-ion batteries during charge and discharge processes causes to increase their temperature. This increase in temperature has two different effects: beneficial effect that causes to improve the efficiency and the performance of the battery and unfavourable effect that decreases their reliability and makes them closer to thermal run a way [3-6]. So, thermal management is crucial to ensure thermal stability and long-term durability of the Li-ion batteries [7].

Between different kinds of thermal management systems, air cooling has attracted the attentions of many researchers due to their simplicity. Giuliano et al. [8] investigated an air-cooled thermal management system for high-capacity Lithium Titanate batteries by fabricating metal-foam based heat exchanger plates and showed that the air-cooled systems can be an effective method for the thermal management of automotive battery packs and require lower power than conventional liquid-cooled systems. Fan et al. [9] computationally investigated an air-cooled module in transient thermal state and found that increasing the air flow rate and lowering the gap spacing, decrease the maximum temperature rise. They also showed that one-side cooling is less effective than two-side cooling for the same gap spacing and airflow rate.

He et al. [10] studied thermal management of Li-ion battery module in a wind tunnel facility and compared the results with that from the CFD simulations. Reasonable agreements between the experimental and CFD results were found. Choi and Kang [11] proposed a simple modelling methodology to describe thermal behaviour of an air-cooled Li-ion battery system and showed that their model can simulate convective heat transfer cooling during battery operation accurately. Fathabadi [12] utilizes several distributed thin ducts for cooling the Li-ion battery pack based on distributed natural convection and illustrated that the proposed battery pack can satisfy all thermal and physical issues relating to the battery packs used in vehicles, and increases the battery life cycle and charge and discharge performances.

Some researchers studied the shape of the battery packs or the battery arrangements inside them. Park [13] modelled a specific design of existing air-cooled battery system and found an appropriate cooling performance could be achieved by employing the tapered manifold and pressure relief ventilation. Xu and He [14] investigated the heat dissipation performance of a battery pack and showed that it improves by changing them from longitudinal state to horizontal state because of shortening the air flow path. Sun and Dixon [15] utilized a three-dimensional battery pack thermal model and analytical DOE (Design of Experiments) approach to identify a design concept of a "Z-type" flow pack and found that the use of tapered inlet and outlet ducts reduces the variation of flow rates of cooling channels. Wang et al. [16] studied thermal performance of a battery module under different cell arrangement structures and found that installing the fan on top of the module has the best cooling performance; cubic arrangement is the most desired structure concerning the cooling effect and cost; and hexagonal structure is optimal according to the space utilization of the battery module.

As temperature uniformity inside the battery is an important parameter that effects on battery life time, some researchers investigated it more precisely. Xun et al. [17] investigated the thermal behaviours of flat-plate and cylindrical batteries and showed that increasing the cooling channel size improves the cooling energy efficiency but decreases the temperature uniformity. Zhongming et al. [18] introduces a shortcut computational method to study a parallel air flow-cooled large battery pack and illustrated that the air flow distribution in the parallel cooling channels was non-uniform, even though the air was distributed by wedge-shaped plenums. Yu et al. [19] designed an air flow integrated thermal management system that contains of two types of air ducts with independent intake channels and fans. The results showed that the maximum temperature can be decreased and temperature uniformity of the battery packs can be enhanced significantly. Mohammadian and

Zhang [20] introduced a special kind of pin fin heat sink whose heights of pin fins increase linearly through the width of the channel; they showed that this kind of pin fin heat sink decreased the standard deviation of the temperature field inside the battery and improved the temperature uniformity.

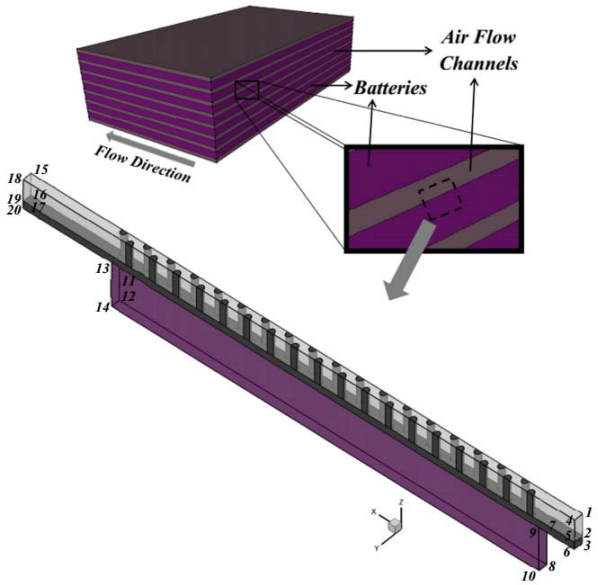

Fig. 1 Schematic of the thermal management system

The goal of thermal management of the Li-ion batteries is preparing a uniform temperature field inside the battery and also preventing to reach the thermal runaway. In this study, three-dimensional transient thermal analysis of an air-cooled module that contains prismatic Li-ion cells next to a heat sink (Fig. 1) was studied to find that whether constant-height pin fin heat sinks which are more applicable for non-battery industries, are appropriate to use for thermal management of Li-ion batteries.

PROBLEM STATEMENT AND HEAT GENERATION IN LI-ION UNIT CELLS

To simplify the simulations, just one symmetrical part of the battery pack was considered to pay more attentions on the temperature variation and uniformity inside the battery. The computational domain was divided to three parts: (1) an inlet part with the length of 6 times of the hydraulic diameter of pin cross section, (2) an outlet part with the length of 15 times of the hydraulic diameter of pin cross section to avoid the effects of backflow streams, and (3) the main part that contains the heat sink and the battery. Boundary conditions were tabulated in Table 1. The optimum gap spacing of 3 mm was considered for air flow channel height [9] and the thickness of aluminium heat sink considered being *0.5* mm between the battery cells. The diameter and heights of the fins were *2* mm and *3* mm, respectively. Staggered arrangement with longitudinal and transverse pitch to diameter ratios of $S_L/d=2$ and $S_T/d=1$ was considered. The dimensions and properties of the prismatic cells were tabulated in Table 2.

Heat generation inside the battery is a complex process that depends on the electrochemical reaction rate that changes with time and temperature [4]. The most commonly used approach to estimate battery heat generation is the correlation proposed by Bernardi et al. [21] which was derived from the thermodynamic energy balance on a complete cell. Simplified form of the Bernardi's correlation is as follow [22]:

Table 1: Boundary Conditions

Boundary Condition	*Section*
Velocity Inlet	*(1-2-5-4)*
Pressure Outlet	*(15-16-19-18)*
Symmetry	*(1-2-16-15), (2-3-17-16), (7-8-12-11), (4-5-19-18), (5-6-20-19), (9-10-14-13), (1-4-18-15), (8-10-14-12)*
Adiabatic Wall	*(2-3-6-5), (7-8-10-9), (3-6-9-7), (16-17-20-19) (11-12-14-13), (11-13-20-17)*

Table 2: Dimensions and properties of the prismatic cells [9]

Dimension or property	*Value*
Active area dimensions (mm)	*6 × 145 × 255*
Density (kg/m3)	*~ 2335*
Specific heat capacity (J/kg K)	*~ 745*
Thermal conductivity (W/m K)	*~ 27 (along surfaces) , ~ 0.8 (in thickness direction)*

$$\dot{Q} = I(U - V) - I\left(T\frac{\partial U}{\partial T}\right) \quad (1)$$

where $\dot{Q}$ is the heat generation rate, I is the electric current passing through the unit cell, U is the open-circuit voltage of the unit cell, V is the cell voltage, and T is the cell temperature. The first term of the right-hand side of Eq. (1) is the irreversible heat generation due to Ohmic losses in the cell, charge-transfer over potentials at the interface, and mass transfer limitations. The second term is reversible heat generation due to entropic changes [23]. It was assumed that there is no phase change or mixing effects and only one electrochemical reaction occurs in the batteries during normal operation.

Equation (1) can be simplified as follow [12, 24, 25]:

$$\dot{q} = R_i i^2 - iT\frac{\Delta S}{F} \quad (2)$$

where $\dot{q}$ is the rate of internal heat generation per unit volume, R_i is the internal equivalent resistance of the unit cell, i is the discharge current of Li-ion unit cell per unit volume, ΔS is the entropy change, and F is the Faraday number (96485 C/mol). The internal equivalent resistance of a unit cell depends on both the temperature and SOC of the battery and was measured as below [12-24]:

$$R_i = \begin{cases} 2.258\times10^{-6}SOC^{-0.3952} & T = 20℃ \\ 1.857\times10^{-6}SOC^{-0.2787} & T = 30℃ \\ 1.659\times10^{-6}SOC^{-0.1692} & T = 40℃ \end{cases} \quad (3)$$

Entropy change is almost independent of the temperature over the range of the temperature between about 18℃ and 42℃ [12,24] and was measured as follow:

$$\Delta S \approx \begin{cases} 99.88\,SOC - 76.67 & 0 \le SOC \le 0.77 \\ -30 & 0.77 \le SOC \le 0.87 \\ -20 & 0.87 \le SOC \le 1 \end{cases} \quad (4)$$

where SOC is defined as:

$$SOC = 1 - \frac{I.t}{C_0} \quad (5)$$

where I is the discharge current, C_0 ($=15Ah$) is the electric capacity of the proposed battery and t is the discharge duration. Thermal radiation was assumed to be negligible in this study.

NUMERICAL SOLUTION

During the past three decades, computational fluid dynamics techniques and codes have been used extensively to design, analyse and optimize the fluid flow devices and processes [9]. In this study, a pressure based, second order transient model in Fluent was employed. As the PISO scheme provides faster convergence for transient flows than the standard SIMPLE approach [26], this scheme has been utilized for the pressure-velocity coupling. For transient problems, the PISO algorithm decrease the number of iterations required for convergence however it takes more CPU time per solver iteration [27]. The convergence is checked by monitoring the scaled residuals. The initial temperature and inlet velocity were considered to be *27 °C* and *0.412 m/s*, respectively. The time step for integrating the governing equations was set to be 1s. The convergence criterion was set such that the residuals of the governing equations for flow and thermal energy were below 10^{-6}. The UDF code was written according to the mentioned correlations and used to calculate the transient heat generation inside the battery.

After creating the plane between the battery and pin fin heat sink, the volumes were created and defined to be pin fins in the case of with pin fins and were considered as part of the fluid flow in the case of without pin fins. To study the grid sensitivity, after testing 3 grid densities, an appropriate grid system of about 1,759,170 cells has been selected for simulation in this study. Fig. 2 shows this computational grid.

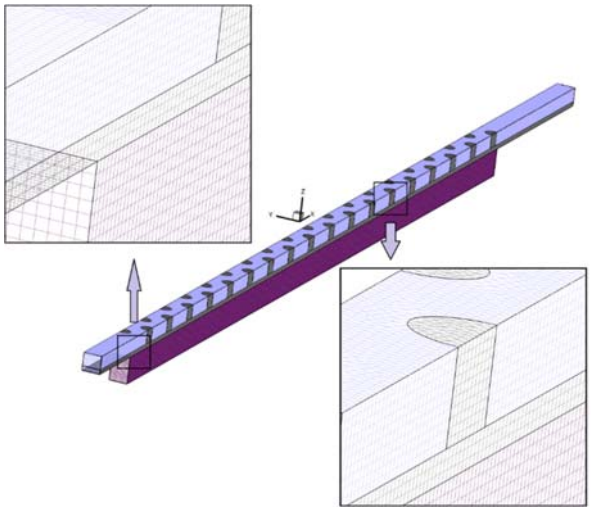

Fig. 2 Computational grid

To validate the simulations of this study, the numerical results by Fan et al. [9] are utilized. The minimum and maximum temperatures of the battery pack extracted from Ref. [9] were considered to evaluate the transient heat generation inside the battery. Next, the constant discharge rate was estimated by the use of evaluated heat generation and was put in the UDF code. The numerical results were obtained at the temperature of *27 °C* and tabulated in Table 3. Good agreements with the maximum error of 2.92% were found between the standard deviation of temperature field inside the battery estimated in this study and Fan et al. [9] at t=600s.

Table 3: Comparison of the standard deviation of the temperature field inside the battery at t=600s

Flow Rate (m^3/h)	*This Study*	*Fan et al. [7]*	*%*
10.2	*0.841*	*0.863*	*2.55*
20.4	*0.832*	*0.823*	*1.08*
30.6	*0.746*	*0.756*	*1.32*
40.8	*0.685*	*0.665*	*2.92*

RESULTS AND DISCUSSIONS

The objective of this work was to illustrate the destructive effect of constant-height pin fin heat sink on the thermal management of Li-ion battery pack. Thermal analysis was performed and the effects of different parameters on thermal performance of the battery were considered.

Figure 3 illustrates the temperature variations close to the top surface of the battery and bottom surface of the heat sink, through the width of the heat sink for the cases of with (right hand side) and without (left hand side) pin fins at SOC=0.167. It can be seen that, through the width of the heat sink for both cases of with and without pin fins, first the temperatures of the battery and fluid increase and after passing the maximum point, they start to decrease. For discharge rates of 1C and 2C the trends show that they have not reached to the maximum points. But for discharge rate of 5C, it is clear that the temperature reaches to the maximum point before passing the outlet of the airflow channel. Also, this figure shows that the use of pin fin heat sink leads to significant decrease in the temperature inside and outside of the battery; especially for the discharge rate of *5C*.

Figure 4 illustrates the maximum temperature and standard deviation of the temperature field inside the battery versus the state of charge for different discharge rates. It is clear that with decreasing the state of charge, both the maximum temperature and standard deviation of the temperature field inside the battery increase. The use of pin fins decreases the maximum temperature inside the battery. However, it increases the standard deviation of the temperature field, which is unfavourable. Figure 4 clearly shows that setting the pin fins on the surface of the heat sink through the width of the battery may decrease the temperature of the battery, but it causes to increase in the standard deviation of the temperature field inside the battery, which affect electrochemical performance of the battery and relatively decreases the efficiency. In the other words, for thermal management of the Li-ion batteries, the priority of the temperature uniformity inside the battery is higher than the priority of decreasing the temperature. Figure 4 also indicated increasing both the maximum temperature and standard deviation of the temperature field with increasing the rate of discharge. By increasing the discharge rate, the heat generation accelerated because the cell shifted from its equilibrium state and hence, this lets to rapid increase of the cell temperature [1].

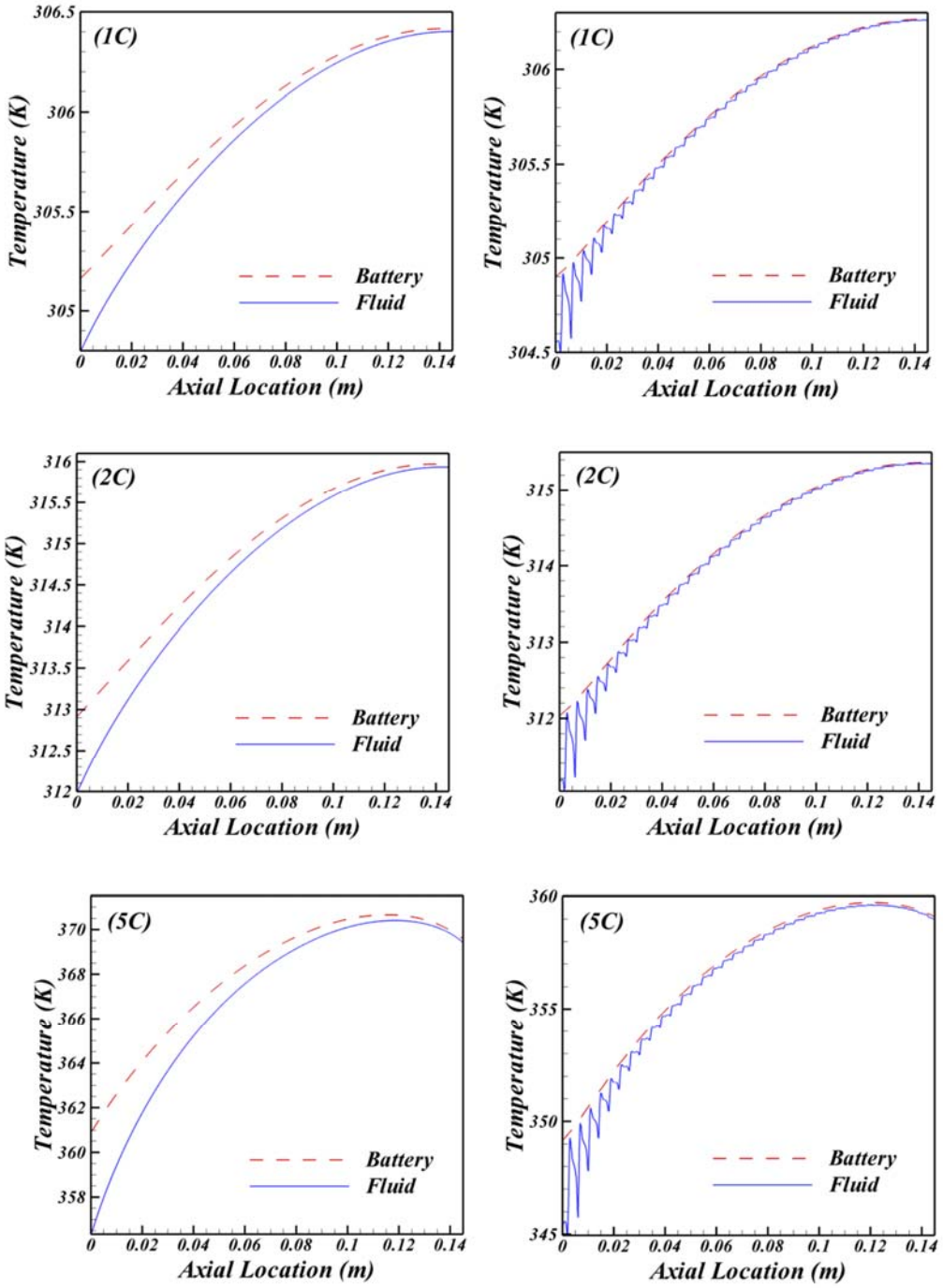

Fig. 3 Temperature variations through the width of the heat sink for with (Right hand side) and without (Left hand side) pin fins (SOC=0.167)

Figure 5 shows the comparison of the temperature distribution inside the battery for the cases of with and without pin fins (SOC=0.667, 2C). It can be seen that although using pin fins causes of significant decrease in temperature inside the battery, it decreases the temperature uniformity inside the battery at the same time. As previously mentioned, the goals of thermal management of the Li-ion batteries are first decreasing the standard deviation of the temperature field (increasing uniformity) and then preventing to reach to thermal runaway; Figure 5 clearly shows that, the use of pin fin heat sink in this condition cannot help us to achieve the first goal of a thermal management system for Li-ion batteries although these kinds of pin fin heat sinks are widely used in many industries and are really beneficial.

Figure 6 shows the value of heat generation inside the battery according to the temperature by the use of Eq. (2). It is clear that with increasing the temperature, heat generation inside the battery decreases; after reaching to the minimum point, it starts to increase. This is because internal equivalent resistance (R_i) decreases with increasing the temperature that causes to decrease

in irreversible heat generation [28]. On the other hand, reversible heat generation increases with increasing temperature. Thus, heat generation inside the battery decreases first because the rate of decreasing the irreversible heat generation is higher than the rate of increasing the reversible heat generation. But after the minimum point, the rate of increasing the reversible heat generation is higher than the rate of decreasing the irreversible heat generation. Figure 7 demonstrates the heat flux contours and temperature distribution in different cross sections for the cases of with and without pin fins (SOC=0.667, 2C). It can be seen that, the use of pin fins increases the rate of heat flux which transfer more heat from the battery. Also, it is clear that, the rate of heat flux decreases along the width of the heat sink. It is because through the width of the heat sink, the temperature difference between the battery and the air flow decreases.

Furthermore, Fig. 7 shows that the isothermal points between the battery and the air flow are near the outlet of the air flow channel (x=140mm). Also, it is clear that the temperature on those areas is higher than the other areas. According to Fig. 6, heat generation in those areas (close to the outlet) is lower than others. So, heat flux on those areas is lower than others.

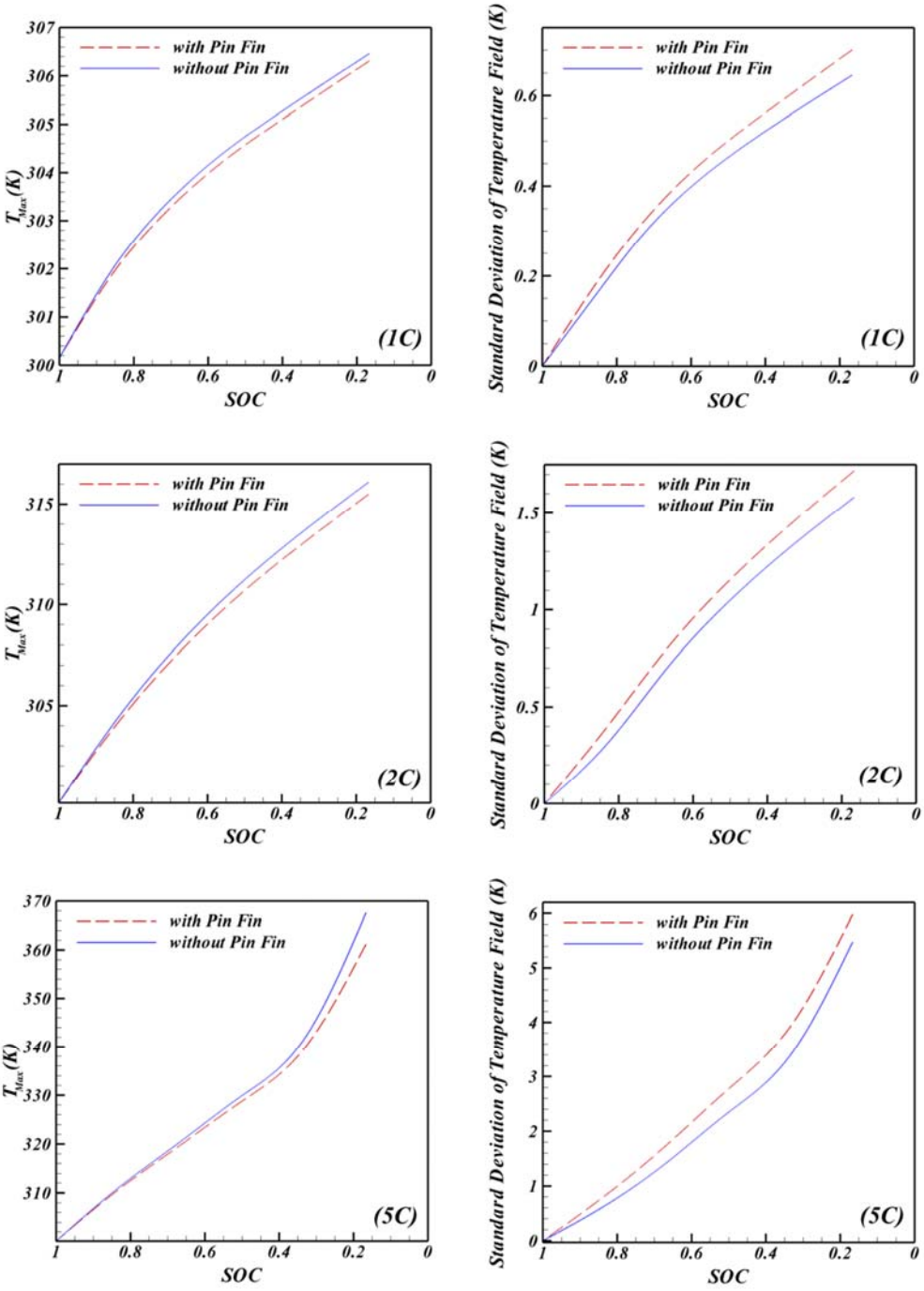

Fig. 4 Maximum temperature inside the battery and standard deviation of temperature field versus SOC

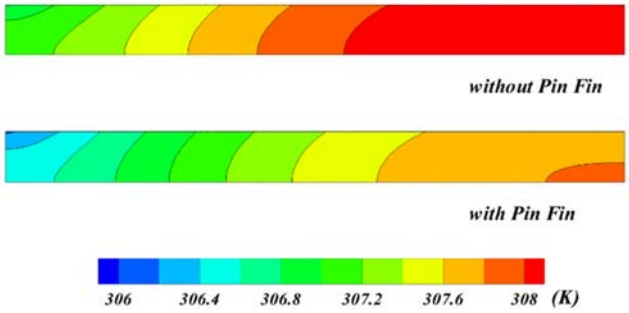

Fig. 5 Comparison of the temperature distribution inside the battery

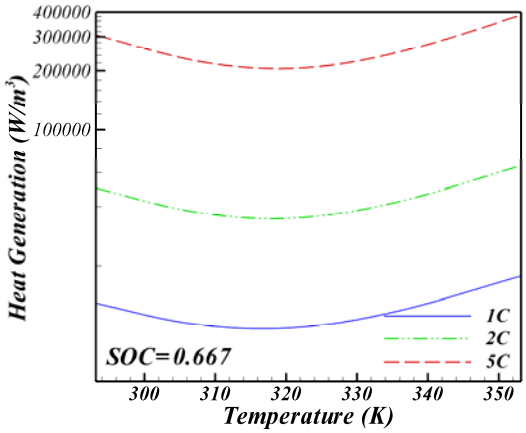

Fig. 6 Heat generation inside the battery versus the temperature

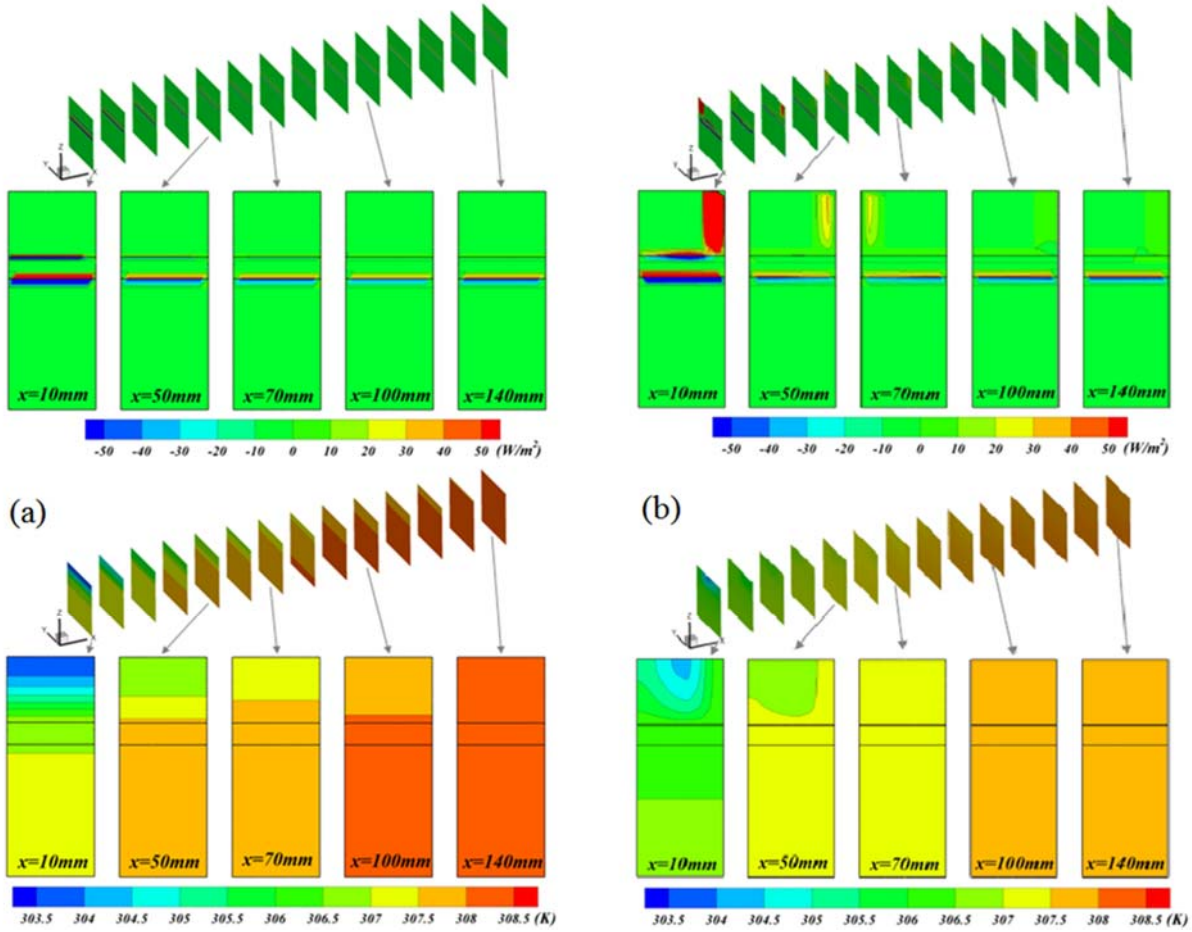

Fig. 7 Heat flux contours and temperature distribution in different cross sections of the battery for the case of (a) without and (b) with pin fins

CONCLUSIONS

Three dimensional transient thermal analysis of an air-cooled module that contains prismatic Li-ion cells next to a heat sink was considered for the cases of with and without pin fins to study the thermal management of Li-ion battery pack. The effects of pin fins, discharge rates, and state of charge on the battery were investigated and the results showed that however the use of pin fin heat sink with constant height significantly leads to decrease the temperature inside the battery, it increases the standard deviation of the temperature filed. As the main goal of a thermal management system for Li-ion batteries is to improve the temperature uniformity inside the battery, so the use of constant-height pin fin heat sink is not beneficial. Also, increasing the discharge rate and decreasing the state of charge cause to increase the temperature inside the battery and worsen the temperature uniformity for both cases of with and without pin fins.

ACKNOWLEDGEMENT

Support for this work by the U.S. National Science Foundation under grant number CBET-1066917 is gratefully acknowledged.

NOMENCLATURE

Symbol	Quantity	SI unit
F	Faraday number	*C/mol*
I	Discharge current of a Li-ion unit cell per unit volume	A/m^3
I	Discharge current	*A*
$\dot{Q}$	Heat generation rate	*W*
$\dot{q}$	Internal heat generation rate per unit volume	W/m^3
R_i	Internal equivalent resistance of unit volume	Ω/m^3
SOC	State of charge	
t	Time duration	*h*
T	Temperature	*°C*
U	Open-circuit voltage	*V*
V	Unit cell voltage	*V*
ΔS	Entropy change	*J/mol K*

REFERENCES

[1] L. H. Saw, Y. Ye, and A. A. O. Tay, Electrochemical-thermal analysis of 18650 lithium iron phosphate cell, Energy Conversion Management 75 (2013) 162-174.

[2] M. R. Giuliano, S. G. Advani, and A. K. Prasad, Thermal analysis and management of lithium-titanate batteries, J. Power Sources 196 (2011) 6517-6524.

[3] D. Lisbona and T. Snee, A review of hazards associated with primary lithium and lithium-ion batteries, Process Safety and Environmental Protection 89 (2011) 434-442.

[4] T. M. Bandhauer, S. Garimella, and T. F Fuller, A critical review of thermal issues in lithium-ion batteries, J. Electrochemical Society 158(3) (2011) R1-R25.

[5] Z. C. Feng and Yuwen Zhang, Thermal runaway due to symmetry breaking in parallel-connected battery cells, Int. J. Energy Research 38 (2014) 813-821.

[6] Z. C. Feng and Yuwen Zhang, Safety monitoring of exothermic reactions using time derivatives of temperature sensors, Applied Thermal Engineering 66 (2014) 346-354.

[7] K. Yu, X. Yang, Y. Cheng, and C. Li, Thermal analysis and two-directional air flow thermal management for lithium-ion battery pack, J. Power Sources 270 (2014) 193-200.

[8] M. R. Giuliano, A. K. Prasad, and S. G. Advani, Experimental study of an air-cooled thermal management system for high capacity lithium-titanate batteries, J. Power Sources 216 (2012) 345-352.

[9] L. Fan, J. M. Khodadadi, and A. A. Pesaran, A parametric study on thermal management of an air-cooled lithium-ion battery module for plug-in hybrid electric vehicles, J. Power Sources 238 (2013) 301-312.

[10] F. He, X. Li, and L. Ma, Combined experimental and numerical study of thermal management of battery module consisting of multiple Li-ion cells, Int. J. Heat and Mass Transfer 72 (2014) 622-629.

[11] Y. S. Choi, and D. M. Kang, Prediction of thermal behaviors of an air-cooled lithium-ion battery system for hybrid electric vehicles, J. Power Sources 270 (2014) 273-280.

[12] H. Fathabadi, A novel design including cooling media for lithium-ion batteries pack used in hybrid and electric vehicles, J. Power Sources 245 (2014) 495-500.

[13] H. Park, A design of air flow configuration for cooling lithium ion battery in hybrid electric vehicles, J. Power Sources 239 (2013) 30-36.

[14] X. M. Xu and R. He, Research on the heat dissipation performance of battery pack based on forced air cooling, J. Power Sources 240 (2013) 33-41.

[15] H. Sun and R. Dixon, Development of cooling strategy for an air cooled lithium-ion battery pack, J. Power Sources 272 (2014) 404-414.

[16] T. Wang, K. J. Tseng, J. Zhao, and Z. Wei, Thermal investigation of lithium-ion battery module with different cell arrangement structures and forced air-cooling strategies, Applied Energy 134 (2014) 229-238.

[17] J. Xun, R. Liu, and K. Jiao, Numerical and analytical modeling of lithium ion battery thermal behaviors with different cooling designs, J. Power Sources 233 (2013) 47-61.

[18] Z. Zhongming, Y. Wang, J. Zhang, and Z. Liu, Shortcut computation for the thermal management of a large air-cooled battery pack, Applied Thermal Engineering 66 (2014) 445-452.

[19] K. Yu, X. Yang, Y. Cheng, and C. Li, Thermal analysis and two-directional air flow thermal management for lithium-ion battery pack, J. Power Sources 270 (2014) 193-200.

[20] S. K. Mohammadian, and Y. Zhang, Thermal management optimization of an air-cooled Li-ion battery module using pin-fin heat sinks for hybrid electric vehicles, J. Power Sources 273 (2015) 431-439.

[21] D. Bernardi, E. Pawlikowski, and J. Newman, A general energy balance for battery systems, J. Electrochemical Society 132(1) (1985) 5-12.

[22] W. B. Gu and C. Y. Wang, Thermal-electrochemical modeling of battery systems, J. Electrochemical Society 147(8) (2000) 2910-2922.

[23] T. M. Bandhauer, Electrochemical-thermal modeling and microscale phase change for passive internal thermal management of lithium ion batteries, Ph.D. dissertation, School Mechanical Engineering, Georgia Institute of Technology (2011).

[24] H. Fathabadi, High thermal performance lithium-ion battery pack including hybrid active-passive thermal management system for using in hybrid/electric vehicles, Energy 70 (2014) 529-538.

[25] G. Karimi and A.R. Dehghan, Thermal management analysis of a Lithium-ion battery pack using flow network approach, Int. J. Mechanical Eng. Mechatronics 1 (2012) 88-94.

[26] ANSYS Inc., Introduction to Ansys Fluent (Lecture 10-Transient flow modeling), Release 13.0 (2010).

[27] D. A. Jones and D. B. Clarke, Simulation of flow past a sphere using the Fluent Code, Australian Government, Department of Defence (Defence Science and Technology Organization) (2008) DSTO-TR-2332.

[28] Y. Inui, Y. Kobayashi, Y. Watanabe, Y. Watase, Y. Kitamura, Simulation of temperature distribution in cylindrical and prismatic lithium ion secondary batteries, Energy Conversion Management 48 (2007) 2103-2109.